


Development of a Spring-Loaded Impact Device to Deliver Injurious Mechanical Impacts to the Articular Cartilage Surface

Cartilage
4(1) 52–62
© The Author(s) 2013
Reprints and permission:
sagepub.com/journalsPermissions.nav
DOI: 10.1177/1947603512455195
http://cart.sagepub.com


Peter G. Alexander^{1,2}, Yingjie Song¹, Juan M. Taboas^{1,2}, Faye H. Chen¹, Gary M. Melvin³, Paul A. Manner⁴, and Rocky S. Tuan^{1,2}

Abstract

Objective: Traumatic impacts on the articular joint surface *in vitro* are known to lead to degeneration of the cartilage. The main objective of this study was to develop a spring-loaded impact device that can be used to deliver traumatic impacts of consistent magnitude and rate and to find whether impacts cause catabolic activities in articular cartilage consistent with other previously reported impact models and correlated with the development of osteoarthritic lesions. In developing the spring-loaded impactor, the operating hypothesis is that a single supraphysiologic impact to articular cartilage *in vitro* can affect cartilage integrity, cell viability, sulfated glycosaminoglycan and inflammatory mediator release in a dose-dependent manner. **Design:** Impacts of increasing force are delivered to adult bovine articular cartilage explants in confined compression. Impact parameters are correlated with tissue damage, cell viability, matrix and inflammatory mediator release, and gene expression 24 hours postimpact. **Results:** Nitric oxide release is first detected after 7.7 MPa impacts, whereas cell death, glycosaminoglycan release, and prostaglandin E2 release are first detected at 17 MPa. Catabolic markers increase linearly to maximal levels after ≥ 36 MPa impacts. **Conclusions:** A single supraphysiologic impact negatively affects cartilage integrity, cell viability, and GAG release in a dose-dependent manner. Our findings showed that 7 to 17 MPa impacts can induce cell death and catabolism without compromising the articular surface, whereas a 17 MPa impact is sufficient to induce increases in most common catabolic markers of osteoarthritic degeneration.

Keywords

articular cartilage, trauma, degeneration, *in vitro* model, mechanical impact, osteoarthritis

Introduction

An estimated 40 million Americans have some form of arthritis or other rheumatic condition. Osteoarthritis (OA), a degenerative joint disease, is the most common form of arthritis, affecting 12.1% of U.S. adults or 20.7 million people.^{1,2} Posttraumatic OA, characterized by erosion of articular cartilage, osteophyte formation, increase in subchondral bone mass, and subchondral bone cysts,³ accounts for 12% of all cases of OA.^{2,4} The cartilage deterioration results from direct mechanical damage to cartilage tissue or indirect injury through joint instability or joint incongruity, all of which produce abnormal or supraphysiologic mechanical forces in the tissue.^{5,6} We are interested in understanding the contribution of direct mechanical cartilage injury to the initiation of posttraumatic OA.

The application of defined loads *in vivo* that induce osteoarthritic changes have been difficult and infrequent with notable exceptions.^{7–13} The greatest challenge has been to quantify the impact in magnitude, speed, and area and

characterize the pathogenesis following the injury to the osteoarthritic condition. The tightly controlled nature of *in vitro* models offers analytical advantages over *in vivo* models by allowing the measurement and manipulation of

¹Cartilage Biology and Orthopaedics Branch, National Institute of Arthritis, and Musculoskeletal and Skin Diseases, National Institutes of Health, Department of Health and Human Services, Bethesda, MD, USA

²Center for Cellular and Molecular Engineering, Department of Orthopaedic Surgery, University of Pittsburgh School of Medicine, Pittsburgh, PA, USA

³Office of Science and Technology, National Institute of Arthritis, and Musculoskeletal and Skin Diseases, National Institutes of Health, Department of Health and Human Services, Bethesda, MD, USA

⁴Department of Orthopaedics and Sports Medicine, University of Washington, Seattle, WA, USA

Corresponding Author:

Rocky S. Tuan, Center for Cellular and Molecular Engineering, Department of Orthopaedic Surgery, University of Pittsburgh, School of Medicine, 450 Technology Drive, Room 221, Pittsburgh, PA 15219, USA
Email: rst13@pitt.edu

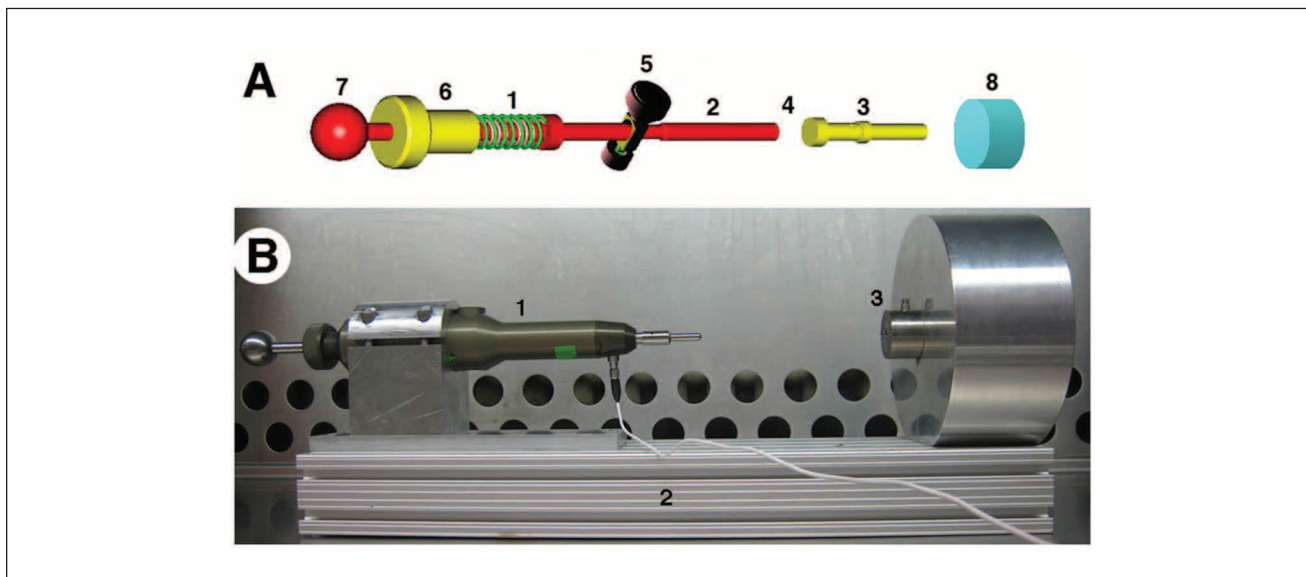


Figure 1. Set up for delivery of mechanical impact to articular cartilage. **(A)** Impactor schematics. Compression of the spring in the load mechanism (**A1**) is controlled by the threaded screw (**A6**; 1 mm compression/turn) mated with the housing of the impactor (not shown). Thus, the force applied to the missile on spring release is linearly related to the turns of the screw. Compression is accomplished by pulling the tensor knob (**A7**) until the release mechanism (**A5**) engages a notch in the piston. Activating the release mechanism (**A5**) releases the piston (**A2**) that collides with the interchangeable impactor missile (**A3**), which ultimately strikes the cartilage (**A8**). The internal load cell (**A4**) is placed in line between the piston (**A2**) and missile (**A3**), and fixed to the latter. There is sufficient travel between the piston and projectile so that the piston does not contact the missile at the time of cartilage impact. **(B)** *Ex vivo* impact of 5 mm cartilage plug, showing impactor (**B1**) with housing clamped to an aluminum armature (**B2**) continuous with the sample chamber (**B3**).

many impact parameters. There are several models of post-traumatic OA that deliver injurious loads to articular cartilage *in vitro*, including drop towers, pendulums, motors, and springs.¹⁴⁻¹⁹ These are all valid means of modeling post-traumatic OA provided the parameters of the impact are representative of those in traumatic impacts that are defined not merely by the magnitude of load but more importantly the rate of force application. Rise times of 1 to 2 ms and loading rates or stress rates greater than 100 kN/s and 1,000 MPa/s, respectively,²⁰ describe impact parameters above those experienced by cartilage or bone *in vivo* during normal activities. Besides variability in the definitions of traumatic impact, these studies are difficult to compare with one another because they employed cartilage from different species, juvenile or adult, isolated from different joints, under different conditions, and often assaying a small, non-overlapping set of outcomes. Despite these variables, taken together these studies have been instructive in characterizing and defining the effect of impacts on cartilage degeneration.^{21,22}

We intended to develop a manually controllable spring-loaded device that delivers a single, well-defined impact load of adjustable magnitude in either an *in vivo* or *ex vivo* laboratory setting to study posttraumatic OA disease progression. Our design included load cells in line within the impacting mechanism to record impact

force and duration of each impact, in combination with measurement of the impact foot print, to allow us to estimate displacement of the impactor. Together, this information provides precise characterization of each impact. The main objectives of this study are (a) to verify that a spring-loaded impact device can be used to deliver traumatic impacts of consistent magnitude and rate and (b) to verify that these impacts cause catabolic changes by analyzing a more comprehensive set of stimuli from a range of impact magnitudes. In testing our spring-loaded impactor, we hypothesize that a single supraphysiologic impact to articular cartilage *in vitro* can affect cartilage integrity, cell viability, and sulfated glycosaminoglycan (GAG) and inflammatory mediator release in a dose-dependent manner. The results will guide future studies using differential injuries to investigate injury mechanisms and treatment protocols.

Materials and Methods

Impactor Design and Use

A custom-engineered, spring-loaded impactor (**Fig. 1A**) was designed to deliver 100 to 2,000 N using interchangeable springs and a smooth, stainless steel hemispherical tip with a radius of 2.5 mm. The compression of the 5-mm spring in

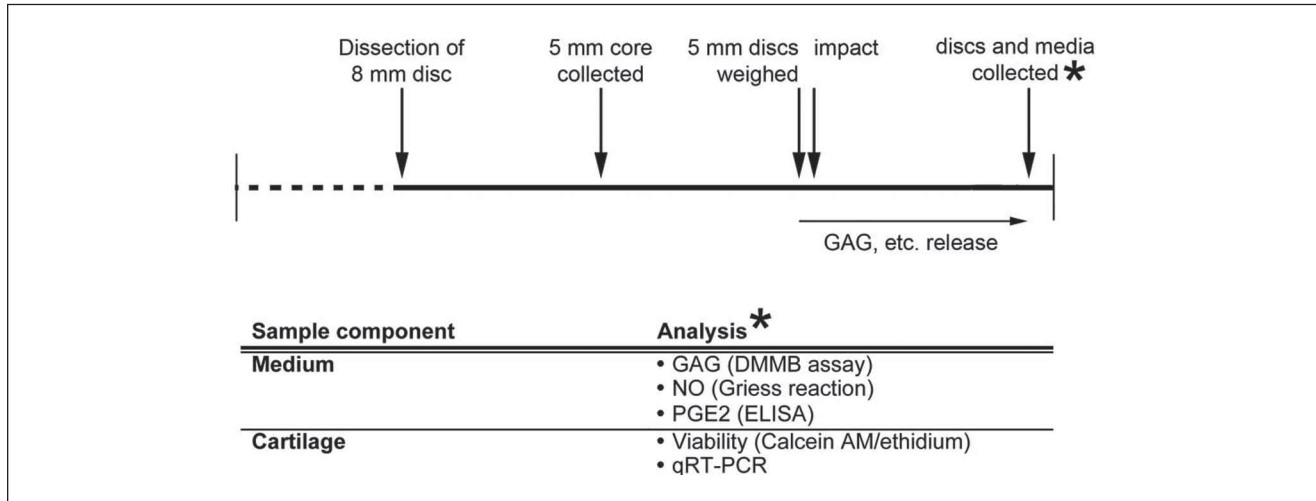


Figure 2. Experimental scheme and time line. Articular cartilage discs 8 mm in diameter were dissected from adult bovine patellofemoral groove 24 hours after slaughter, allowed to equilibrate in chondrogenic medium (CM) for 24 hours, at which time the final 5 mm diameter core was removed. After an additional 24 hours, the 5-mm discs were weighed and checked for a regular geometry before sorting and impact. After impact, samples were returned to CM and cultured for 24 hours when the cartilage discs and media were collected. One set of samples was immediately stained for cell viability, and the other processed for gene expression by quantitative reverse transcriptase polymerase chain reaction (qRT-PCR).

the load mechanism is controlled by the threaded screw (1 mm compression/turn) mated with the housing of the impactor (**Fig. 1A**). Thus, the force applied to the missile on spring release is linearly related to the turns of the screw. Importantly, the design of the device allowed for sufficient travel between the piston and projectile so that the piston does not contact the missile at the time of cartilage impact. Although originally intended for hand-held use, a fixation device was added to clamp the impactor and an *ex vivo* sample chamber to create a rigid system (**Fig. 1B**). Impact forces were recorded with two 10 to 200 lb quartz force sensors (QFG 200, Cooper Instruments, Warrendale, VA), one fitted in line between the internal piston and impactor projectile (**Fig. 1A**) and another underneath the cartilage sample. Force profiles were sampled at 200 kHz using a signal conditioner model QSC 484 (Cooper Instruments), an analog-to-digital converter model NI-9215 (BNC-USB; National Instruments Corp., Austin, TX), and LabView 7.0 software (National Instruments). Force curves were analyzed in Microsoft Excel (Redmond, WA). Impact area, defined as the maximum tissue surface area contacted by the hemispherical projectile tip during an impact motion, was measured using medium sensitivity Fuji Pressurex pressure-sensitive film (Sensor Products, Inc., East Hanover, NJ) placed between the impactor tip and the articular surface. Impact footprints were digitally scanned using a Microtek flatbed scanner, rendered in Adobe Photoshop CS2 (Adobe, San Jose, CA) and analyzed for geometry using NIH ImageJ 1.62.

Experimental design. Articular cartilage discs 5 mm diameter and 1.8 to 2.2 mm in thickness were subjected to one

impact in a range of impact forces produced by increasing the spring compression in 1 mm increments (5-10 mm compression). The samples were allowed to incubate in medium for 24 hours after impact before the medium was collected for GAG, nitrite, and PGE2 release, while the cartilage disc is processed in one of two ways. One group was bisected and analyzed for cell viability through the impact region, whereas the other group will be processed for gene expression analysis. The experimental scheme is summarized in **Figure 2**.

Application of Impact

Articular cartilage explants were isolated from the patellofemoral groove of the hind-leg stifle of 2- to 3-year-old bovine within 24 hours of slaughter (JW Trueth and Sons, Baltimore, MD). In brief, 8-mm circles were scored in the articular surface with a steel biopsy punch. The cartilage disc was removed from the subchondral bone with a scalpel and immediately placed in basal medium (BM: Dulbecco's Modified Eagle's Medium [DMEM], 10% fetal bovine serum [FBS; Atlanta Biological, Lawrenceville, GA], and penicillin/streptomycin/fungizone). After 24 hours, a central 5-mm core was removed from the 8-mm disc and cultured in 1 ml of serum-free chondrogenic medium (CM; phenol-free DMEM, ITS [10 mg/L insulin, 55 mg/L transferrin, 6.7 mg/L selenium], antibiotic/antimycotic solution, [penicillin/streptomycin/amphotericin], 40 mg/ml proline, 50 mg/L ascorbate, 100 mg/ml sodium pyruvate, 10 mM HEPES, and 10 ng/ml recombinant human transforming growth factor- β [TGF- β 3]).²³ After weighing, samples

Table 1. Impact Parameters of Spring-Loaded Device

Spring Compression (mm)	Time to Peak (ms)	Peak Force (N)	Normalized Peak Impact Stress (MPa)	Maximum Displacement (Strain) (%)	Spring Potential Energy (J)	Loading Rate to Peak Force (103) (N/s)	Average Stress Rate (103) (MPa)	Average Strain Rate (103) (%/s)
0.010	0.49 ± 0.02	553.27 ± 50.5	40.84 ± 2.48	38.17 ± 3.51	0.343	1120 ± 50	82.6 ± 2.5	77.2 ± 3.5
0.009	0.47 ± 0.02	453.52 ± 82.1	36.05 ± 5.62	38.55 ± 3.54	0.278	970 ± 82	77.1 ± 5.62	82.5 ± 3.5
0.008	0.52 ± 0.02	379.57 ± 32.3	32.13 ± 1.93	33.81 ± 3.35	0.220	736 ± 32	62.3 ± 1.	65.6 ± 3.4
0.007	0.61 ± 0.04	259.11 ± 34.8	27.57 ± 3.17	27.48 ± 2.12	0.168	426 ± 35	45.4 ± 3.2	45.2 ± 2.1
0.006	0.82 ± 0.02	117.48 ± 12.0	17.23 ± 1.57	18.97 ± 1.69	0.123	144 ± 12	21.2 ± 1.6	23.3 ± 1.7
0.005	0.96 ± 0.10	24.75 ± 5.06	7.65 ± 1.06	6.81 ± 0.84	0.086	26 ± 5	8.0 ± 1.1	7.1 ± 0.8

Seventeen impact profiles analyzed per spring compression.

between 2.2 and 1.80 mm in thickness were randomly distributed into seven different impact load magnitude groups from 0.0 to 40 MPa. Samples were equilibrated for 24 hours in CM. On the day of the experiment, the cartilage samples were placed in the impact chamber, 5 mm in diameter and 2.2 mm deep, covered with a piece of polyvinyl-enclosed, medium sensitivity Fuji Pressurex film, and subjected to the desired level of impact force. Impacted samples were returned to wells containing fresh CM and allowed to incubate for 24 hours.

Histological Analysis

After impact, five to seven samples for each impact load were collected and stained with India ink to mark the fissure for photographic recording with a Qimaging™ Micropublisher CCD camera (Bumbay, BC, Canada) mounted on a Leica dissecting microscope. After bisecting transversely through the impact zone, one half of each sample was paraformaldehyde-fixed, paraffin-embedded, and 8-mm sections prepared for histological analysis. Stains used included Safranin O (Sigma, St Louis, MO), Fast Green (Vector Laboratories, Burlingame, CA), hematoxylin (Rowley Biochemical, Danvers, MA) and eosin (Rowley Biochemical), Alcian Blue, pH 1.0 (Rowley Biochemical), and Nuclear Red (Vector Laboratories, Burlingame, CA).

Cell Death Analysis

The second half of the impacted cartilage samples was immersed in Live/Dead detection medium (2 μM calcein AM, 4 μM ethidium homodimer; Invitrogen, San Diego, CA) for 30 minutes at 37 °C and washed in phosphate-buffered saline (PBS). Images of epifluorescently illuminated (488 nm/520 nm; 493 nm/635 nm) samples were recorded, imported into NIH ImageJ 1.62, and live/dead cells were

counted manually using fixed selection parameters for either 488 or 520 nm channels.

Sulfated Glycosaminoglycan Analysis

Impacted tissue samples ($n = 17$; three experiments) were washed in PBS and digested in 1 ml/mg cartilage of papain (200 mg papain/ml in 5 mM L-cysteine, 100 mM sodium acetate, 100 mM Na₂HPO₄, 10 mM EDTA, pH 6.4.) at 55 °C for 24 hours or until completely digested. After 5 or 10-fold dilution, GAG was detected using the Blyscan™ assay (BiColor, Carrickfergus, Ireland). For GAG in the medium, 100 μL of medium was papain digested in 900 μL of buffer for 2 hours at 55 °C and assayed using Blyscan method.

Nitric Oxide and Prostaglandin E2 Analyses

Stored frozen medium from each sample ($n = 9$; two experiments) in an impact group was used to measure nitric oxide (NO) and prostaglandin E2 (PGE2) release. For NO quantitation, 50 μL of medium was assayed in triplicate employing the Promega Griess Reaction Kit (Promega, Sunnyvale, CA). For PGE2 quantitation, 150 μL of medium was analyzed using the PGE2 ELISA kit (R&D Systems).

Quantitative RT-PCR

Gene Expression Analysis

Cartilage plugs from each impact force group ($n = 5$; two experiments) were flash-frozen and powderized in liquid. Total RNA was extracted with Trizol (Invitrogen, San Diego, CA) and further purified using RNeasy Cleanup Kit clean-up kit (Germantown, MD). First-strand cDNA synthesis was performed using Superscript III™ (Invitrogen), and real-time polymerase chain reaction (PCR) was conducted with gene-specific primers (Table 1) and SYBR

Green (Invitrogen) using an iCycler thermocycler (BioRad, Hercules, CA) and data analyzed using the manufacturer's software. mRNA expression levels were normalized to GAPDH.

Statistical Analysis

One-way ANOVA analysis was used to analyze differences between experimental groups and statistical significance attributed when $P < 0.05$. Variance is reported in the measured and calculated values describing the impact in **Table 1**.

Results

Impactor Design and Impact Characterization

We set out to design a hand-held impactor to deliver traumatic impact loads similar to those that occur in sports and automobile accidents with the following characteristics: an impact time less than 2 ms and a loading rate greater than 100 kN/s. The projectile tip size was selected to deliver stress rates greater than 1,000 MPa/s and/or strain rates greater than 500/s.²⁰ In our spring-based system, the theoretical maximum energy delivered on impact, assuming frictionless elastic collision of the two moving masses (piston and projectile) within the device, is the potential energy stored in the spring, given by the equation $E = \frac{1}{2}kx^2$, where k is the spring constant, x is the change in spring length, and E is the energy. Medium-grade pressure-sensitive film was placed between the impacting tip and the cartilage surface to record the area of the impact and corroborate load cell readings. (Note: Of various films tested, the medium paper provided maximum signal to noise while capturing a large percentage [$>90\%$] of the impacted area; data not shown). Pressure-sensitive film contact footprint was used to calculate the maximum displacement of the cartilage by the impactor tip modeled as a sphere striking a flat surface. A hemispherical end was employed for the impactor tip after initial studies revealed this shape to produce the most consistent impact geometry, particularly when applied to the curved articular surface (data not shown). We used a 5-mm-long spring set with a total compression constant of 6,860 N/m as it delivered the desired force magnitude using a 10-mm spring compression range. **Table 1** shows the resulting impact characteristics of strikes using spring compressions between 5 and 10 mm compression on cartilage plugs 5 mm in diameter and 1.8 to 2.2 mm in thickness in confined compression. Several characteristics of the impact profiles were noted. The peak load delivered (40.84 MPa) exceeded loads known to fracture cartilage, whereas the lowest load (7.65 MPa) was in the range of those experienced physiologically. The load rate was consistently above 100 kN/s, a characteristic of traumatic impact

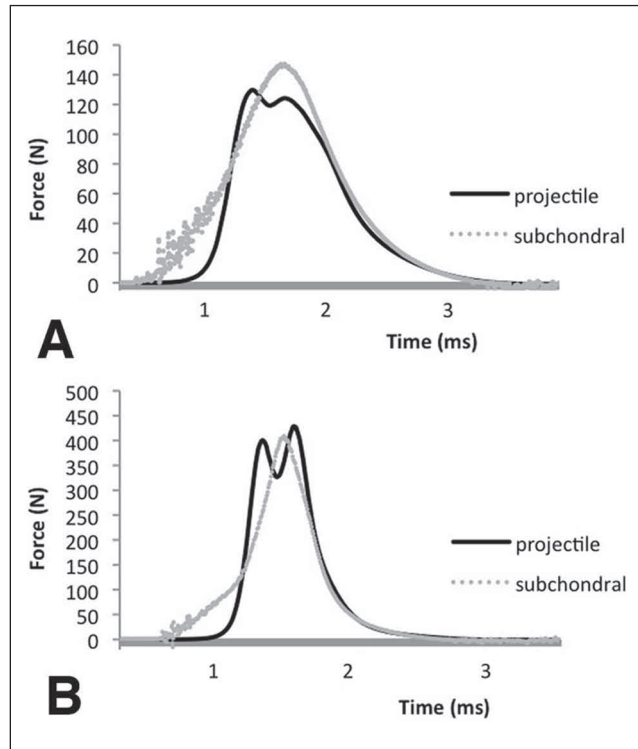


Figure 3. Comparison of force-versus-time data recorded by the projectile-mounted force sensor and the subchondrally mounted sensor for a typical impact generated by (A) 9 mm or (B) 6 mm compression of a spring ($k = 6,860 \text{ m}^2/\text{s}^2$) striking a 2.0 mm thick \times 5 mm diameter plug of bovine articular cartilage in confined compression.

loads,²⁰ except in the case of the lowest spring compression tested (5 mm). The average time-to-peak (ttp) of the impacts ranged between 0.49 and 0.96 ms, resulting in average stress rates consistently above the 1,000 MPa/s benchmark. The maximum estimated displacement, calculated from the diameters of the footprint and impactor tip, ranged between 38.17% for the highest force impacts and 6.81% for the lowest, serving only as an indicator that the cartilage was experiencing greater strain with increased load. In all, the strain rate was above 500%/s, a key feature of traumatic impacts.²⁰ Because the calculated load is dependent on the impact footprint and there is anticipated nonlinearity in the pressure paper-detected footprint-to-force relationship, these values served only as a guide.

An examination of the impact force/time profiles recorded by the internal projectile-mounted sensor revealed two peaks (**Fig. 3**). Using the 36 MPa (9 mm spring compression) impact as an example (**Fig. 3A**), the two peaks are separated by 200 to 300 ms later. We interpreted the second peak to represent the impact on the cartilage. An examination of the subchondrally mounted sensor reveals a single impact of about 1.8 ms and a ttp of approximately 0.8 to 0.9 ms,

indicating the cartilage experiences the 200 to 300 ms doublet impact as a single blow. As impact loads are decreased, the total impact times and ttp become longer, but the essential features of the doublet recorded by the projectile-mounted sensor and the singlet recorded by the subchondral sensor remain unchanged (**Fig. 3B**).

Postimpact Tissue Morphology and Cell Death

Fissuring of the articular surface began at impact loads of 17.2 MPa (0.12 J; 4/12 samples fissured) with all samples fissuring at 27.57 MPa (0.17 J; 12/12 samples fissured) as detected by India ink staining (data not shown). Quantitative analysis (**Fig. 4G**) revealed significant cell death following impact loads of 17.2 MPa (0.12 J) or greater and significant increases in death relative to this threshold at 27.57 MPa (0.17 J). Cell death occurred in the surface zones and along the margins of fissures (**Fig. 4A-F**). At impact loads above 36.0 MPa (0.28 J), cell death in the transition zone appeared more prevalent.

Impact-Mediated Increases in GAG, PGE₂, and Nitrite Release

Impact application on the articular cartilage plugs also resulted in significant changes to the cartilage extracellular matrix and biochemical responses in the chondrocytes. GAG analysis of culture medias showed significant detectable change following impacts of 17.2 MPa (0.12 J) over unimpacted samples (**Fig. 5A**). At greater loads, GAG release continued to trend upwards, with a significant increase from 17.2 MPa results at 40.84 MPa (0.34 J). A consistent trend in increased PGE₂ production over unimpacted samples was also observed with increasing impact magnitude, with the first significant rise at 27.6 MPa (**Fig. 5B**). A significant detectable rise in nitrite release into the medium 24 hours after impact was observed at 7.7 MPa (0.09 J) (**Fig. 5C**), a load slightly lower than that observed for either GAG or PGE₂ release.

Impact-Mediated Changes in Gene Expression

Chondrocyte response to impact was further analyzed on the basis of gene expression profiles. Quantitative RT-PCR analysis of gene expression of catabolic enzymes and extracellular matrix proteins was carried out on unimpacted cartilage, and cartilage subjected to low impact (17.23 MPa) and high impact forces (36.0 MPa) (**Fig. 6**). Twenty-four hours after impact, high-impact loads produced significant increases in MMP3 and 9, whereas MMP13 and aggrecanase 2 (ADAM-TS5) expression remained unchanged (**Fig. 6B**). The expression of cartilage extracellular matrix genes, collagen type II and aggrecan, were

slightly affected and trended downward compared with unimpacted samples. On the other hand, 24 hours after low-impact loads, MMP3 was unchanged, whereas MMP9 and 13 expressions were increased (**Fig. 6A**). For both impact groups, ADAM-TS5 as well as collagen type II and aggrecan were relatively unchanged compared with unimpacted controls.

Discussion

We report here the design and performance parameters of a spring-loaded impacting device with a spherical impact geometry for the purpose of studying the effect of supra-physiological impact on articular cartilage. This impactor consistently delivers a range of impacts, that is, loads between 7 and 41 MPa with other variables such as impact time, area, and displacement changing accordingly. Our impactor shares similarities in design to previous devices.¹⁴ Our innovation with respect to the spring-loaded device is the inclusion of a 100 kHz load cell incorporated in line with the impactor piston and missile to record in real time the force and duration of the impact delivered. This allows us to characterize each impact more precisely. We also record the impact footprint of each impact using pressure-sensitive film so that load can be calculated, and an estimated maximum displacement, a value proportionally related to strain, can be calculated when the cartilage thickness is taken into account. In this study, we have locked the impactor in an armature continuous with the sample chamber to minimize energy loss through movement of the impactor or sample. Measurement of biological outputs showed that impacts at 17.6 MPa routinely induced cartilage fissuring and significantly increased detectable cell death and GAG release, suggesting that this magnitude may be an injury threshold for traumatic impacts. Increases in NO and PGE₂ release at 7.7 MPa and 27.6 MPa, respectively, may reflect the differing roles these inflammatory mediators have in response to injury. The release of these inflammatory mediators and altered gene expression profiles may lead to the development of OA degeneration of the articular cartilage after traumatic articular impact *in vivo*.

The biological responses of the adult bovine chondral plugs to the range of impact magnitudes applied are qualitatively similar to those reported using drop towers,^{16,19,24-28} pendulums,²⁹ and motorized^{18,30-34} and spring-loaded devices.¹⁴ Quantitative differences between the results of this study and previous work may relate to one or more factors, including the magnitude and rate of the impact,³⁰⁻³⁴ the use of juvenile cartilage,^{24,32} the inclusion of subchondral bone,^{14,19,26,29,33-35} the use of confined versus unconfined compression^{19,25,30,36} or whole joint components,^{24,27,28} and the geometry of the impacting surface.^{14,19,25,26,35,36} Our study distinguishes itself in that a variety of biological responses by isolated cartilage are simultaneously

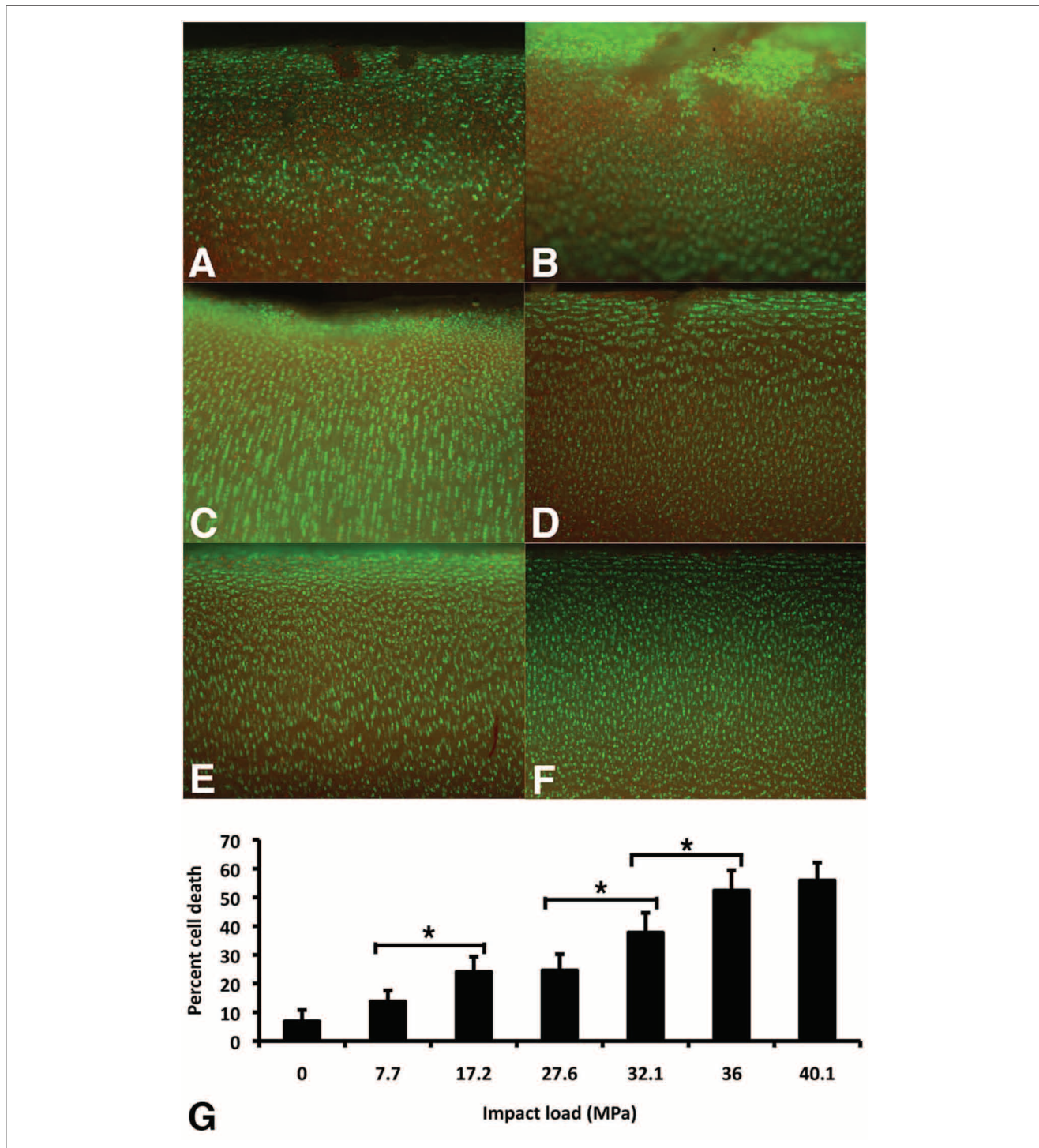


Figure 4. Cell death in cartilage plugs as a result of impact. (A-F) Epifluorescence images of cartilage samples impacted at indicated loads. Twenty-four hours after impact, samples were bisected transversely, stained with calcein-AM (green) for living cells and ethidium homodimer (red) for dead cells. Bar = 0.5 mm. (G) Quantitation of dead cells as a percentage of total cell number. Digital images were imported into Image J and standardized thresholds applied for circularity and emission intensity before the ratio of dead to total cell number was calculated. Values are the mean \pm SD of five samples from one experiment (*, $P < 0.01$).

assayed over a range of impacts in order to reveal a more comprehensive view of the early posttraumatic impact mechanisms.

The analysis reported here showed two impact magnitudes, 17 (low) and 36 MPa (high), that are both traumatic but lead to potentially different catabolic processes. Impacts

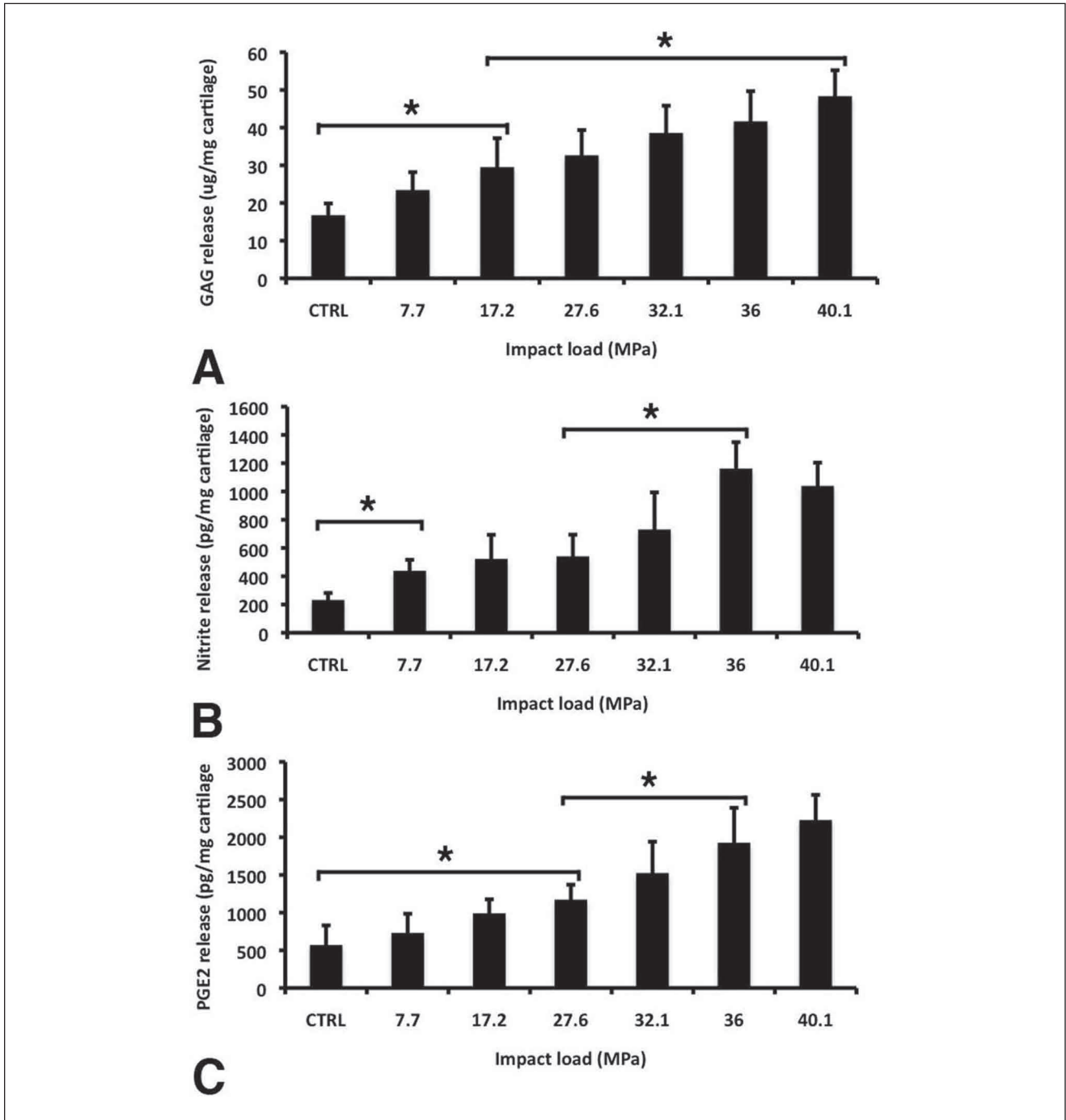


Figure 5. Markers of cartilage degeneration and inflammation detected in the medium of cartilage plugs 24 hours after being impacted at different impact loads. **(A)** Glycosaminoglycan (GAG) was measured using the DMMB-based Blycan assay. **(B)** Prostaglandin E2 (PGE2) was measured by ELISA. **(C)** Nitrite release was measured using the Griess reagent system (NED reduction). Values are the mean \pm SD of 13 **(A)** or 9 **(B and C)** samples from three independent experiments (*, $P < 0.01$).

at 17 MPa show a statistically significant increase in all biochemical markers over control unimpacted samples, whereas 36 MPa impacts result in a maximal per cell response. On the molecular level, we found that among the limited number of genes analyzed, lower injurious impact

loads resulted in increases in MMP9 and MMP13, whereas high injurious impact loads increased MMP9 and MMP3. Similar changes in catabolic gene expression have been reported in osteoarthritis³⁷ and mechanically injured cartilage.³⁸ Other catabolic genes such as MMP1 and ADAM-TS5,

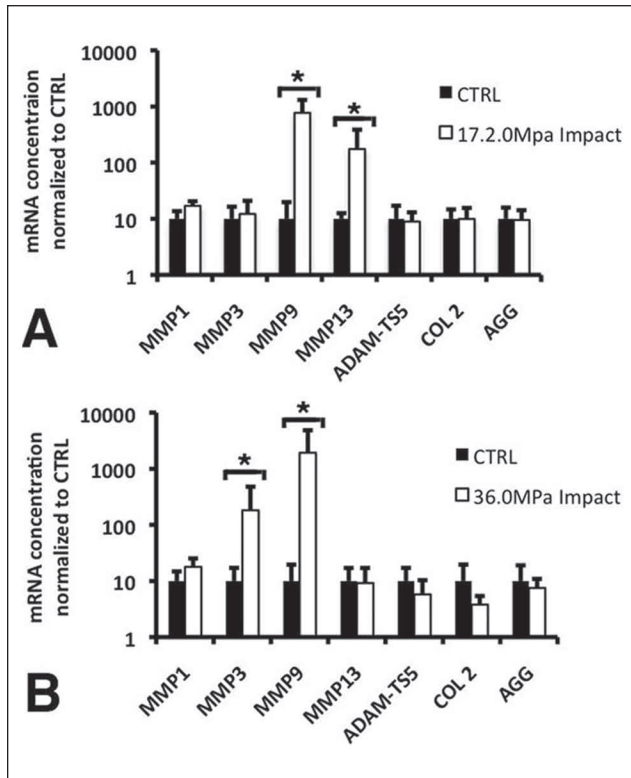


Figure 6. Expression of selected matrix components, MMPs, and aggrecanases detected by qRT-PCR in cartilage plugs 24 hours after being impacted at either (A) 36.1 ± 5.6 MPa or (B) 17.2 ± 1.6 MPa. Values are the mean \pm SD of five samples per data point from two independent experiments normalized to GAPDH expression (*, $P < 0.01$).

as well as the cartilage matrix genes aggrecan and collagen type II, were statistically unchanged. This difference may be the result of different level of tissue damage and differing integrin/MAPK responses to mechanical disruption and resultant cytokine release. Integrins are important in chondrocyte sensing and response to load,^{39,40} and their expression is changed in OA.⁴⁰⁻⁴³ Stimulation of these integrin complexes induces NO.^{44,45} A titration of the impact load forces required for *in situ*, integrin-mediated NO, and its relation to subsequent cartilage degeneration has not been explored. There is a statistical difference in NO release between the two impacts employed here (3.38 vs. 24.47 pg/mg cartilage). NO is one of the prominent mediators of stress response, both following physiological loads and injurious loads, and it is hypothesized in many systems that the level of NO (and other mediators) may be critical in the difference between a controlled repair response and a degenerative destruction of tissue.⁴⁵ Our analysis is limited to a short time point (24 hours) and only at the mRNA levels, not enzyme activities. However, our findings are consistent with previously reported impact-mediated changes in cartilage metabolism.¹⁹

In conclusion, these experiments represent a rigorous test and validation of a manually controllable spring-loaded device for the delivery of traumatic impacts to the articular cartilage surface that results in structural, biochemical, and molecular changes consistent with the initiation of degenerative changes within the tissue. In future studies, the application and consequences of this impact protocol in long-term cultures *in vitro* and in an animal model *in vivo* will be studied.

Acknowledgments and Funding

Supported in part by the Intramural Research Program of the NIH (Z01 AR41131) and the Commonwealth of Pennsylvania Department of Health (SAP 4100050913).

Declaration of Conflicting Interests

The author(s) declared no potential conflicts of interest with respect to the research, authorship, and/or publication of this article.

Ethical Approval

This research was carried out in accordance with the guidelines found in Guide for the Care and Use of Laboratory Animals, 8th edition.

References

- Buckwalter JA, Martin JA. Osteoarthritis. *Adv Drug Deliv Rev.* 2006;58(2):150-67.
- Felson DT. An update on the pathogenesis and epidemiology of osteoarthritis. *Radiol Clin North Am.* 2004;42(1):1-9.
- Brandt KD, Dieppe P, Radin EL. Etiopathogenesis of osteoarthritis. *Rheum Dis Clin North Am.* 2008;34(3):531-59.
- Brown TD, Johnston RC, Saltzman CL, Marsh JL, Buckwalter JA. Posttraumatic osteoarthritis: a first estimate of incidence, prevalence, and burden of disease. *J Orthop Trauma.* 2006;20(10):739-44.
- Buckwalter JA, Martin JA, Brown TD. Perspectives on chondrocyte mechanobiology and osteoarthritis. *Biorheology.* 2006;43(3-4):603-9.
- Kerin A, Patwari P, Kuettner K, Cole A, Grodzinsky A. Molecular basis of osteoarthritis: biomechanical aspects. *Cell Mol Life Sci.* 2002;59(1):27-35.
- Borrelli J Jr, Burns ME, Ricci WM, Silva MJ. A method for delivering variable impact stresses to the articular cartilage of rabbit knees. *J Orthop Trauma.* 2002;16(3):182-8.
- Haut RC, Ide TM, De Camp CE. Mechanical responses of the rabbit patello-femoral joint to blunt impact. *J Biomech Eng.* 1995;117(4):402-8.
- Newberry WN, Mackenzie CD, Haut RC. Blunt impact causes changes in bone and cartilage in a regularly exercised animal model. *J Orthop Res.* 1998;16(3):348-54.
- Newberry WN, Zukosky DK, Haut RC. Subfracture insult to a knee joint causes alterations in the bone and in the functional stiffness of overlying cartilage. *J Orthop Res.* 1997;15(3):450-5.

11. Radin EL, Paul IL, Pollock D. Animal joint behaviour under excessive loading. *Nature*. 1970;226(5245):554-5.
12. Torzilli PA, Grigiene R, Borrelli J Jr, Helfet DL. Effect of impact load on articular cartilage: cell metabolism and viability, and matrix water content. *J Biomech Eng*. 1999;121(5):433-41.
13. Vrahas MS, Smith GA, Rosler DM, Baratta RV. Method to impact in vivo rabbit femoral cartilage with blows of quantifiable stress. *J Orthop Res*. 1997;15(2):314-7.
14. Bolam CJ, Hurtig MB, Cruz A, McEwen BJ. Characterization of experimentally induced post-traumatic osteoarthritis in the medial femorotibial joint of horses. *Am J Vet Res*. 2006;67(3):433-47.
15. Borrelli J Jr, Zhu Y, Burns M, Sandell L, Silva MJ. Cartilage tolerates single impact loads of as much as half the joint fracture threshold. *Clin Orthop Relat Res*. 2004;(426):266-73.
16. Jeffrey JE, Gregory DW, Aspden RM. Matrix damage and chondrocyte viability following a single impact load on articular cartilage. *Arch Biochem Biophys*. 1995;322(1):87-96.
17. Krueger JA, Thisse P, Ewers BJ, Dvoracek-Driksna D, Orth MW, Haut RC. The extent and distribution of cell death and matrix damage in impacted chondral explants varies with the presence of underlying bone. *J Biomech Eng*. 2003;125(1):114-9.
18. Milentijevic D, Helfet DL, Torzilli PA. Influence of stress magnitude on water loss and chondrocyte viability in impacted articular cartilage. *J Biomech Eng*. 2003;125(5):594-601.
19. Natoli RM, Scott CC, Athanasiou KA. Temporal effects of impact on articular cartilage cell death, gene expression, matrix biochemistry, and biomechanics. *Ann Biomed Eng*. 2008;36(5):780-92.
20. Aspden RM, Jeffrey JE, Burgin LV. Impact loading of articular cartilage. *Osteoarthritis Cartilage*. 2002;10(7):588-9.
21. Martin JA, Buckwalter JA. Post-traumatic osteoarthritis: the role of stress induced chondrocyte damage. *Biorheology*. 2006;43(3-4):517-21.
22. Roach HI, Aigner T, Soder S, Haag J, Welkerling H. Pathobiology of osteoarthritis: pathomechanisms and potential therapeutic targets. *Curr Drug Targets*. 2007;8(2):271-82.
23. Mauck RL, Yuan X, Tuan RS. Chondrogenic differentiation and functional maturation of bovine mesenchymal stem cells in long-term agarose culture. *Osteoarthritis Cartilage*. 2006;14(2):179-89.
24. Atkinson TS, Haut RC, Altiero NJ. Impact-induced fissuring of articular cartilage: an investigation of failure criteria. *J Biomech Eng*. 1998;120(2):181-7.
25. Burgin LV, Aspden RM. A drop tower for controlled impact testing of biological tissues. *Med Eng Phys*. 2007;29(4):525-30.
26. D'Lima DD, Hashimoto S, Chen PC, Colwell CW Jr, Lotz MK. Impact of mechanical trauma on matrix and cells. *Clin Orthop Relat Res*. 2001;(391 Suppl):S90-S99.
27. Duda GN, Eilers M, Loh L, Hoffman JE, Kaab M, Schaser K. Chondrocyte death precedes structural damage in blunt impact trauma. *Clin Orthop Relat Res*. 2001;(393):302-9.
28. Repo RU, Finlay JB. Survival of articular cartilage after controlled impact. *J Bone Joint Surg Am*. 1977;59(8):1068-76.
29. Broom ND. Structural consequences of traumatizing articular cartilage. *Ann Rheum Dis*. 1986;45(3):225-34.
30. Ewers BJ, Dvoracek-Driksna D, Orth MW, Haut RC. The extent of matrix damage and chondrocyte death in mechanically traumatized articular cartilage explants depends on rate of loading. *J Orthop Res*. 2001;19(5):779-84.
31. Lewis JL, Deloria LB, Oyten-Tiesma M, Thompson RC Jr, Ericson M, Oegema TR Jr. Cell death after cartilage impact occurs around matrix cracks. *J Orthop Res*. 2003;21(5):881-7.
32. Loening AM, James IE, Levenston ME, Badger AM, Frank EH, Kurz B, et al. Injurious mechanical compression of bovine articular cartilage induces chondrocyte apoptosis. *Arch Biochem Biophys*. 2000;381(2):205-12.
33. Morel V, Quinn TM. Short-term changes in cell and matrix damage following mechanical injury of articular cartilage explants and modelling of microphysical mediators. *Biorheology*. 2004;41(3-4):509-19.
34. Quinn TM, Allen RG, Schalet BJ, Perumbuli P, Hunziker EB. Matrix and cell injury due to sub-impact loading of adult bovine articular cartilage explants: effects of strain rate and peak stress. *J Orthop Res*. 2001;19(2):242-9.
35. Milentijevic D, Torzilli PA. Influence of stress rate on water loss, matrix deformation and chondrocyte viability in impacted articular cartilage. *J Biomech*. 2005;38(3):493-502.
36. Jeffrey JE, Aspden RM. Cyclooxygenase inhibition lowers prostaglandin E2 release from articular cartilage and reduces apoptosis but not proteoglycan degradation following an impact load in vitro. *Arthritis Res Ther*. 2007;9(6):R129.
37. Aigner T, Zien A, Gehrsitz A, Gebhard PM, McKenna L. Anabolic and catabolic gene expression pattern analysis in normal versus osteoarthritic cartilage using complementary DNA-array technology. *Arthritis Rheum*. 2001;44(12):2777-89.
38. Lee JH, Fitzgerald JB, Dimicco MA, Grodzinsky AJ. Mechanical injury of cartilage explants causes specific time-dependent changes in chondrocyte gene expression. *Arthritis Rheum*. 2005;52(8):2386-95.
39. Ramage L, Nuki G, Salter DM. Signalling cascades in mechanotransduction: cell-matrix interactions and mechanical loading. *Scand J Med Sci Sports*. 2009;19(4):457-69.
40. Millward-Sadler SJ, Salter DM. Integrin-dependent signal cascades in chondrocyte mechanotransduction. *Ann Biomed Eng*. 2004;32(3):435-46.
41. Holledge MM, Millward-Sadler SJ, Nuki G, Salter DM. Mechanical regulation of proteoglycan synthesis in normal and osteoarthritic human articular chondrocytes—roles for alpha5 and alphaVbeta5 integrins. *Biorheology*. 2008;45(3-4):275-88.
42. Pulai JI, Del Carlo M Jr, Loeser RF. The alpha5beta1 integrin provides matrix survival signals for normal and osteoarthritic human articular chondrocytes in vitro. *Arthritis Rheum*. 2002;46(6):1528-35.
43. Salter DM, Millward-Sadler SJ, Nuki G, Wright MO. Differential responses of chondrocytes from normal and osteoarthritic

- human articular cartilage to mechanical stimulation. *Biorheology*. 2002;39(1-2):97-108.
44. Chowdhury TT, Akanji OO, Salter DM, Bader DL, Lee DA. Dynamic compression influences interleukin-1beta-induced nitric oxide and prostaglandin E2 release by articular chondrocytes via alterations in iNOS and COX-2 expression. *Biorheology*. 2008;45(3-4):257-74.
45. Abramson SB. Osteoarthritis and nitric oxide. *Osteoarthritis Cartilage*. 2008;16(Suppl 2):S15-S20.